4-th International Meeting on
Cavitation and Dynamic Problems in Hydraulic Machinery and Systems,
October, 26-28, 2011, Belgrade, Serbia

Non-Linear Stability Analysis of a Reduced Scale Model Pump-Turbine at Off-Design Operation

Christian Landry, Sébastien Alligné, Vlad Hasmatuchi,
Steven Roth, Andres Mueller, François Avellan

EPFL, Laboratory for Hydraulic Machines
Avenue de Cour 33bis, 1007 Lausanne, Switzerland

christian.landry@epfl.ch, sebastien.alligne@epfl.ch, vlad.hasmatuchi@epfl.ch
steven.roth@epfl.ch, andres.mueller@epfl.ch, francois.avellan@epfl.ch

Abstract

Nowadays, the pump-storage power plants are a proven solution for storing electricity at large scale and offering flexibility to the power management. Therefore, the hydraulic machines are increasingly subject to off-design operation, start-up and shutdown sequences. However, the fast and frequent switching between pumping mode and generating mode presents technical challenges.

In the present study, the reduced scale model of a low specific speed pump-turbine $(\nu = 0.12)$ is investigated in generating mode at off-design conditions. The operation in the typical "S-shaped" curve of pump-turbine may become unstable and the machine may switch back and forth from generating mode to reverse pumping mode preventing the correct experimental survey of this part during the model testing. The instability has been solved by a testing procedure imposing a restriction of section and a control valve for being able to increase the energy losses. This procedure, commonly used in model testing of pump-turbines, significantly improves the stability of the machine and allows for the survey of the entire "S-curve".

The aim of the present investigation is to understand and explain the origin of the switch to reverse pumping mode. Thus, a hydro-acoustic test rig model was developed with the In-house EPFL SIMSEN software and a comparison between the systems with and without a restriction of section was studied. A numerical analysis indicates that the operating points of a pump-turbine system are defined by the solution of the equation relating the test rig characteristic and the energy-discharge characteristic of the hydraulic machine for a given rotational speed and a constant guide vanes opening. Furthermore, the addition of a restriction alters the curvature of the test rig characteristic and creates a new degree of freedom to achieve stable operating points in the "S-curve". Finally, to ensure the stability of each operating points described by the numerical model, an eigenvalue study of the non-linear hydraulic system is necessary.

Keywords: Pump-Turbine, Off-design Operation, Instability, Hydro-acoustic Eigenvalues, Numerical investigation

1. Introduction

The behavior of regulated pump-turbines is usually described by a set of characteristic curves [1] Q_{ED}-n_{ED} for flow and T_{ED}-n_{ED} for shaft torque. Furthermore, high head pump-turbines are commonly of the low specific speed types and, therefore, present "S-shaped" characteristic curves. In the literature, many authors have shown that low specific speed pump-turbines with "S-shaped" characteristics near runaway can experience unstable behavior during load rejection. It has been analytically proven by Martin [2], using inelastic theory, that stability can be related to the slope $[dT_{ED}/dn_{ED}]_{\text{runaway}} < 0$ at runaway. Martin [3] concluded that this slope for the low specific speed pump-turbine at runaway is positive for the moderate and large openings, yielding unstable operating conditions. The instability can be directly related to head-discharge curves with negative slopes at the runaway point, which translates to positive slopes in the T_{ED}-n_{ED} plane. Dörfler [4] solved the instability problem by changing the start-up procedure. So, the inlet valve is partially open and by-passed with a second valve to adjust the discharge. This procedure is widely used to allow for the survey of the entire "S-shaped" characteristic. The resulting artificial head loss significantly improves the hydraulic stability.

This paper presents a numerical simulation study of the transient behavior of the HYDRODYNA pump-turbine mounted on the EPFL PF3 test rig. Briefly, once the runaway condition has been reached, the operation becomes unstable and the machine may switch back and forth from generating mode to reverse pumping mode. A new pipe imposing a large restriction of section and equipped with a second valve is then used to avoid the instability and to allow exploring the entire "S-Curve". In the first part of the paper, the modeling of hydraulic components based on equivalent electrical scheme representation is presented. Then, the numerical model is calibrated and validated in order to better describe the physical behavior of systems with and without a restriction of section. Subsequently, the head-discharge curves are analyzed for both models to predict whether the new operating points of the system are in a generating mode or reverse pumping mode. Finally, a study of eigenvalues defines the stability of operating points.

2. Experimental case study

The reduced scale of a low specific speed pump-turbine is tested in the EPFL PF3 test rig shown in Fig.1. Two 400 kW centrifugal pumps connected in series features a maximum head of 100 m and a maximum discharge of 1.4 m^3/s. Moreover, a restriction of section is imposed between the pipes L18 and L20 imposing a reduction of diameter by a factor of 6. Finally, the Iris and butterfly valves force the flow to go either through the pipe L19 or through the restriction.

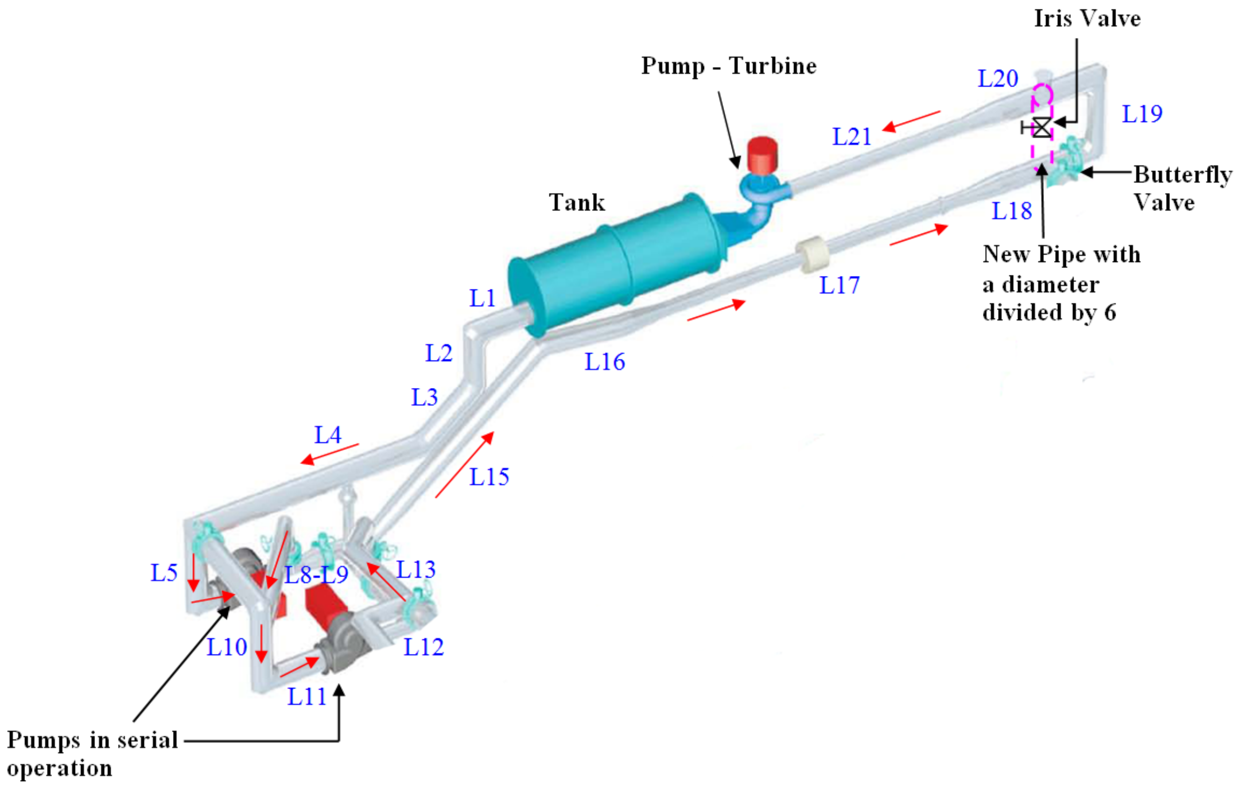

Fig. 1 Sketch of the EPFL PF3 test rig

Off-design conditions involving runaway and "S-shape" turbine brake curve were investigated by Hasmatuchi et al. [5]. The Q_{ED}-n_{ED} and T_{ED}-n_{ED} characteristic curves for the low specific speed pump-turbine are presented in Fig.2 for the small and moderate openings. These curves were divided by the measured data at the best efficiency point (BEP), reported at the test head. At 10° guide vanes opening, the T_{ED}-n_{ED} characteristic curve indicates a positive slope at runaway. When a pump-turbine is operated in such a situation, the operation suddenly switches to reverse pumping mode. The discharge as well as torque and power are reversed with a substantial increase of structural vibrations driven by flow instabilities. A specific procedure, commonly used in model testing of pump-turbine was adopted to stabilize the machine operation: once the runaway is reached, the butterfly valve is closed forcing the flow to go through the restriction and the Iris valve is used to finally adjust the head. This procedure significantly improves the stability of operation by introducing an additional hydraulic resistance and allows the experimental survey of the entire "S-curve".

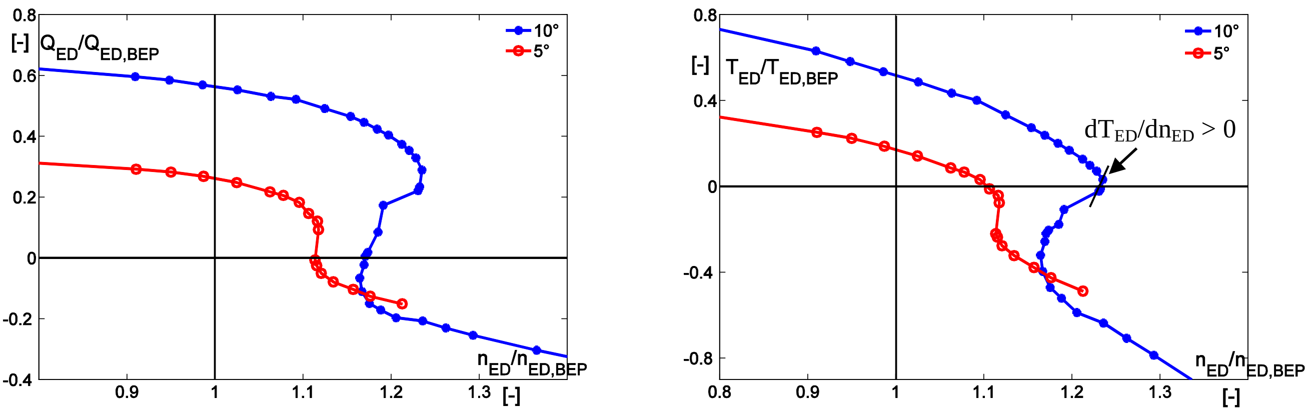

Fig. 2 Q_{ED}-n_{ED} and T_{ED}-n_{ED} characteristic curves of the pump-turbine for 5° and 10° guide vanes openings

3. SIMSEN Model

The modeling of the hydraulic components based on equivalent scheme representation is presented in this section. The following set of hyperbolic partial differential equations describes the one-dimensional momentum and continuity balances for an elementary pipe of length dx and wave speed a. Moreover, we assume uniform pressure and velocity distributions in the cross section A and we neglect the convective terms [6].

$$\begin{cases} \dfrac{\partial h}{\partial t} + \dfrac{a^2}{gA} \cdot \dfrac{\partial Q}{\partial x} = 0 \\ \dfrac{\partial h}{\partial x} + \dfrac{1}{gA} \cdot \dfrac{\partial Q}{\partial t} + \dfrac{\lambda |Q|}{2gDA^2} \cdot Q = 0 \end{cases} \tag{1}$$

The system (1) is solved using the Finite Difference Method with 1st order centered scheme discretization in space and a scheme of Lax for the discharge variable. This discretization leads to a system of ordinary differential equations that can be represented as a T-shaped equivalent scheme [7] as presented in Fig. 3.

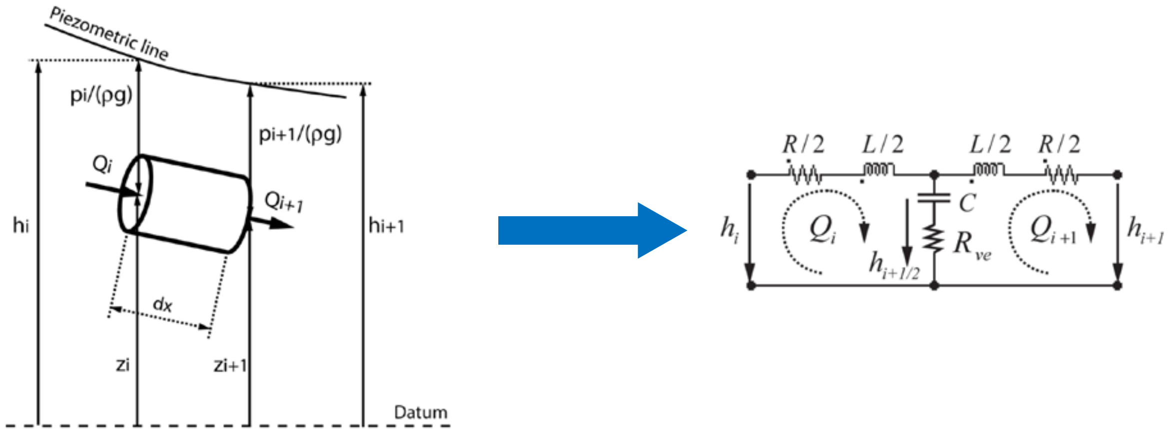

Fig. 3 Representation of an elementary hydraulic pipe of length *dx* and his equivalent circuit

The RLC parameters of the equivalent scheme are given by:

$$R = \frac{\lambda |\overline{Q}| dx}{2gDA^2}, \qquad L = \frac{dx}{gA}, \qquad C = \frac{gAdx}{a^2} \tag{2}$$

where λ is the local loss coefficient and D is the diameter of the elementary pipe. The hydraulic resistance R, the hydraulic inductance L and the hydraulic capacitance C correspond respectively to energy losses, inertia and storage effects. Moreover, in order to predict accurately pressure fluctuation amplitudes and system stability, it is necessary to take into account the viscoelastic behavior due to energy dissipation during the wall deflection. This additional dissipation leads to a resistance in series with the capacitance. This viscoelastic resistance is accounting for both fluid and pipe material viscoelasticity and can be expressed as:

$$R_{ve} = \frac{\mu_{equ}}{A\rho g dx} \tag{3}$$

with μ_{equ} the equivalent viscoelastic damping of both the fluid and the wall. The model of a pipe with a length L is made of a series of elements based on the equivalent scheme illustrated in Fig. 3, the system of equations being set up using Kirchhoff laws. As presented in Tab. 1, the modeling approach based on equivalent electrical schemes of hydraulic components is extended to all the standard hydraulic components such as valves, surge tanks, air vessels, cavitation development, Francis pump-turbines, Kaplan turbines, pumps, etc. Moreover, models of all those components are implemented in the EPFL software SIMSEN, developed for the simulation of the dynamic behavior of hydroelectric power plants [8].

Tab. 1 Modeling of hydraulic components with related equivalent schemes

Hydraulic Components		SIMSEN Objects	Electrical equivalent schemes	Parameters
Generalized pipe	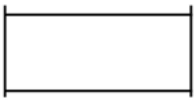		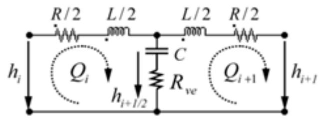	$R = \frac{dx\lambda\lvert Q\rvert}{2gDA^2}$ $R_{ve} = \frac{\mu}{\rho gAdx}$ $L = \frac{dx}{gA}$ $C = \frac{dxgA}{a^2}$
Valve	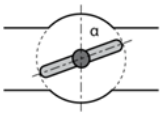	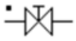	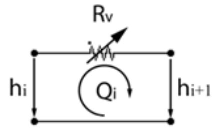	$R_v = \frac{K_v(\alpha)\lvert Q\rvert}{2gA^2}$
Surge tank	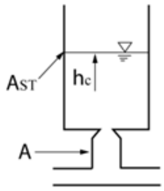		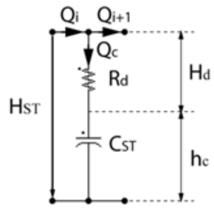	$R_d = \frac{K_d(Q)\lvert Q\rvert}{2gA^2}$ $C_{ST} = A_{ST}(h_c)$
Francis pump-turbine	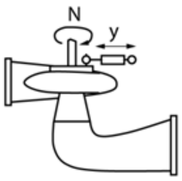		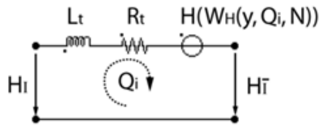	$H = H(W_H(y,Q,N))$ $T = T(W_B(y,Q,N))$ $R_t = R_t(W_H(y,Q,N))$ $L_t = \frac{l_{equ}}{gA}$

W_H : turbine head characteristic [-] l_{equ} : turbine equivalent length [m]
W_B : turbine torque characteristic [-] μ : viscosity of the fluid or material [Pa·s]

The diagram of the SIMSEN model for EPFL PF3 test rig is represented in Fig. 4. To simplify the geometric complexity of the test rig, the following assumptions have been made:

- First, the draft tube is divided into two independent parts: the cone and the diffuser; these components are represented as small pipes with a constant section.
- Then, as the 1D model does not take into account the geometric variations of the circuit, every elbow is described as a singular specific energy loss.
- Finally, the two pumps are hold at constant rotational velocity during the experiment and, therefore, are modeled by two sources of pressure.

To reduce the uncertainty of the system head losses due to assumptions, the pressure source value has been adjusted to obtain the same initial experimental value for a guide vanes opening α_O and a speed of rotation n. In case with the restriction of section, the geometrical modification alters the system head losses and the pressure source value has to be readjusted. The experimental and the numerical values of the IEC factors n_{ED}, Q_{ED} and T_{ED} without the restriction of section are compared in table 2. The low relative uncertainty indicates a good calibration of the numerical model.

Tab. 2 Comparison between the experimental and numerical IEC factors n_{ED}, Q_{ED} and T_{ED} without the restriction of section

	Units	*Experimental Value*	*Numerical Value*	*Relative uncertainty*
$n_{ED} / n_{ED,BEP}$	[-]	1.235	1.233	0.13 %
$Q_{ED} / Q_{ED,BEP}$	[-]	0.305	0.298	2.39 %
$T_{ED} / T_{ED,BEP}$	[-]	0.038	0.038	0.25 %

$$n_{ED} = \frac{n \cdot D}{\sqrt{E}}, \qquad Q_{ED} = \frac{Q}{D^2\sqrt{E}}, \qquad T_{ED} = \frac{T}{D^3 E} \tag{4}$$

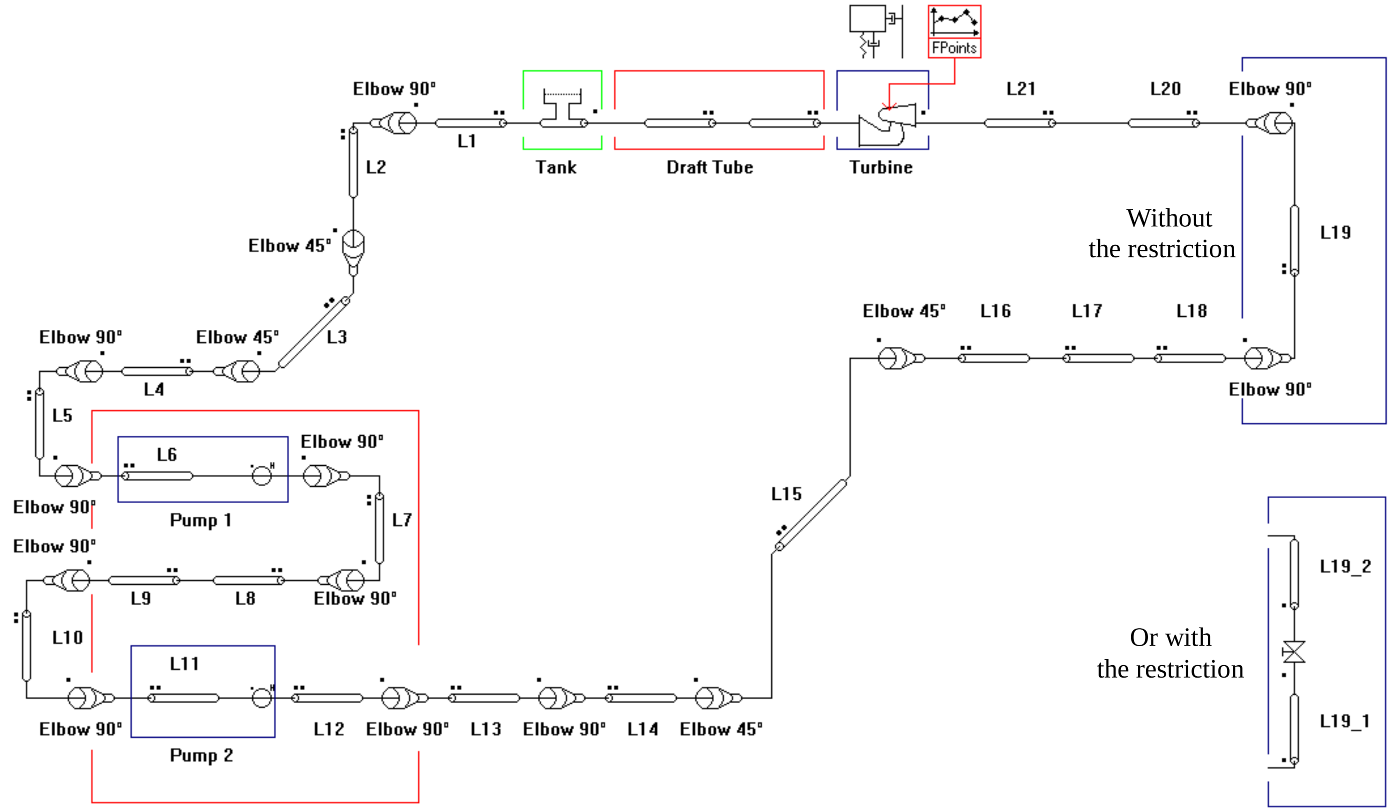

Fig. 4 The diagram of the SIMSEN model for EPFL PF3 test rig with and without restriction of section

4. Stationary operating points

The static equilibrium defined by eq. (5) indicates the stationary operating points of a pump-turbine system at the intersection between respectively the energy-discharge characteristic of the hydraulic machine and the parabola describing the test rig characteristic.

$$E(Q) = \left(gH_I - gH_{\bar{I}}\right)(Q) \tag{5}$$

The evolution of these characteristic curves for constant guide vanes opening and rotational speed are presented in Fig. 5.a and 5.b.

- The characteristic curve of the machine in blue is derived from experimental data n_{ED}-Q_{ED}. Indeed, for the same guide vanes opening, the operating curve depends on the couple of points (n_{ED}, Q_{ED}), the speed of rotation *n* and the runner outlet diameter *D*.

$$E_{pump-turbine} = \left(\frac{n \cdot D}{n_{ED}}\right)^2 \text{ and } \quad Q = Q_{ED} \cdot D^2 \cdot \sqrt{E_{pump-turbine}} \tag{6}$$

- The red characteristic curve represents the evolution of the head losses H_r in the hydraulic circuit. The quadratic relation describing this curve is defined for pumping mode and generating mode as follows:

$$\begin{cases} \left(gH_I - gH_{\bar{I}}\right)_{\text{turbine mode}} = 2E_{pump} - \sum_{i=1}^{n} gH_r = 2E_{pump} - \dfrac{8Q^2}{\pi^2}\sum_{i=1}^{n}\dfrac{K_{v,i}}{D_i^4} & \text{if } Q > 0 \\ \left(gH_I - gH_{\bar{I}}\right)_{\text{pump mode}} = 2E_{pump} + \sum_{i=1}^{n} gH_r = 2E_{pump} + \dfrac{8Q^2}{\pi^2}\sum_{i=1}^{n}\dfrac{K_{v,i}}{D_i^4} & \text{if } Q < 0 \end{cases} \tag{7}$$

The intersection between these characteristic curves corresponds to the solution of the eq.5 and defines the stationary operating points of the system for a given rotational speed and a constant guide vanes opening. Such a representation allows for direct determination of problematic rotational speeds at which a switch of operation from generating to reverse pumping mode is unavoidable.

The initial system without the restriction of section are represented in Fig. 5.a. after increasing the rotational speed of a few revolutions per minute (from $n/n_{BEP}^{*} = 123.2\%$ to 123.5 %). The stability is only reached for a negative discharge imposing a switch to reverse pumping mode. Indeed, a slight increase in the rotational speed shifts the characteristic curve of the machine upwards and prevents an intersection between the hydraulic system curve and the pump-turbine curve in generating mode.

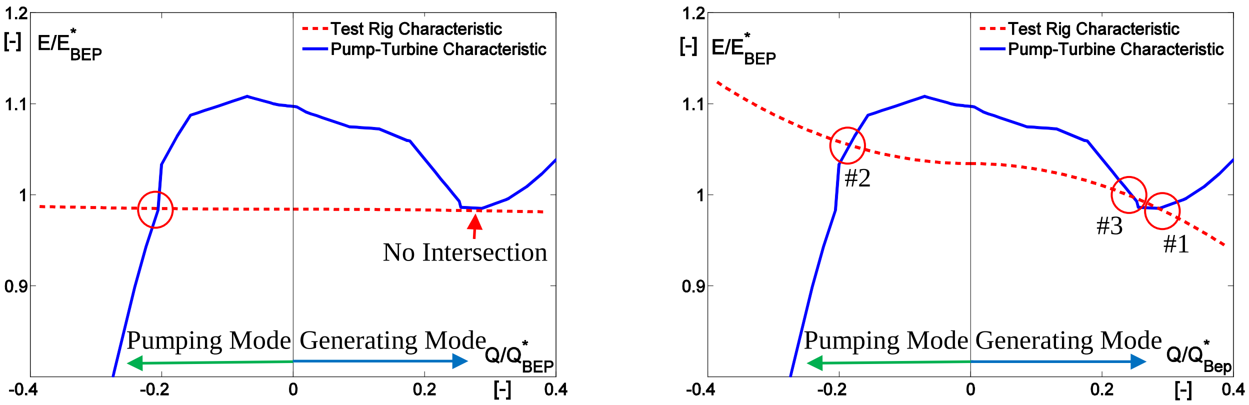

a) Without the restriction of section **b)** With the restriction of section

Fig. 5 Evolution of the specific energy versus the discharge for the turbine and the hydraulic system for $\frac{n}{n^*_{BEP}} = 123.5\%$

However, for the system with the restriction of section (Fig. 5.b), the increase of head losses in the hydraulic circuit enables to reach new points of operation. Point #1 indicates the operating point reached by the system in a turbine mode. This point prevents a reverse flow as well as the onset of vibrations in the pump-turbine. Point #2 describes the operating point in the reverse pumping mode. This one is reached for the same rotational velocity if the system is initially used in reverse pumping mode. Point #3 indicates an unstable point of operation for the hydraulic system. Indeed, the numerical model cannot be stabilized around this point; the hydraulic balance will be established only at the points #1 or #2.

Eventually, the operating points are defined by a system with two degrees of freedom. On the one hand, the modification of the head imposed by the pump causes a vertical translation of the test rig characteristic curve. On the other hand, the restriction of section alters the curvature of the test rig characteristic curve to create an intersection with any point on the operating curve. Thus, a small graphic study can determine what would be the minimal restriction of the section to ensure an operating point in generating mode for a given rotational speed and a constant guide vanes opening.

5. Stability analysis with eigenvalues during transient behavior

The solution of the eq.5 generates, in most cases, three operating points: the first located in turbine mode, the second in pump mode, and the last located in the S-curve. To check the stability for each of them, an eigenvalue study of the non-linear hydraulic system for different time during transient behavior of the pump-turbine was conducted.

The electrical analogy of the hydraulic model describes the dynamic behavior as a first order differential equation system in the matrix form:

$$[A]\frac{d\vec{x}}{dt} + \left[B\left(\vec{x}\right)\right]\cdot\vec{x} = \vec{V}\left(\vec{x}\right) \tag{8}$$

where $[A]$ and $[B(\vec{x})]$ are the state global matrices of dimension $[n \times n]$, $\vec{x}$ and $\vec{V}(\vec{x})$ are respectively the state vector and the boundary conditions vector with n components. The hydraulic resistance R (eq. 2) present in the matrix $[B]$ depends on the discharge Q. Therefore, the multiplication with the state vector $\vec{x}$ can lead to nonlinear terms. The linearization of the system of equation [9] is described by the following relation, where linearized $[B]$ becomes $[B_l]$:

$$[A]\frac{d\cdot\delta\vec{x}}{dt} + [B_l]\cdot\delta\vec{x} = \vec{0} \tag{9}$$

The eigenvalues $s_k = \sigma_k + j\omega_k$ of the system can be calculated from the following characteristic equation:

$$\det\left([\mathrm{I}]s + [A]^{-1}[B_l]\right) = 0 \tag{10}$$

The real part corresponds to the damping σ while the imaginary part corresponds to the pulsation of oscillation ω. A negative real part reveals stable behavior and a positive real part reveals unstable behavior. The eigenvalues were computed for different time during transient behavior of the pump-turbine. In few words, the rotational speed remains constant during the first 20 seconds to check the stability of the model. Then, the rotational speed is increased linearly in five seconds from $n/n^*_{BEP} = 123.2\%$ to $123.5\ \%$, imposing a switch to reverse pumping mode if the system has no restriction of section. Finally, after 30 seconds, the system is stabilized at a new operating point. Thus, at each time step, the real part of all eigenvalues must be negative to ensure stability of the machine. The time history of the real parts for the first two eigenmodes and the evolution of the dimensionless torque T/T^*_{BEP} for each time step between 20 and 30 seconds are represented in Fig. 6.a.

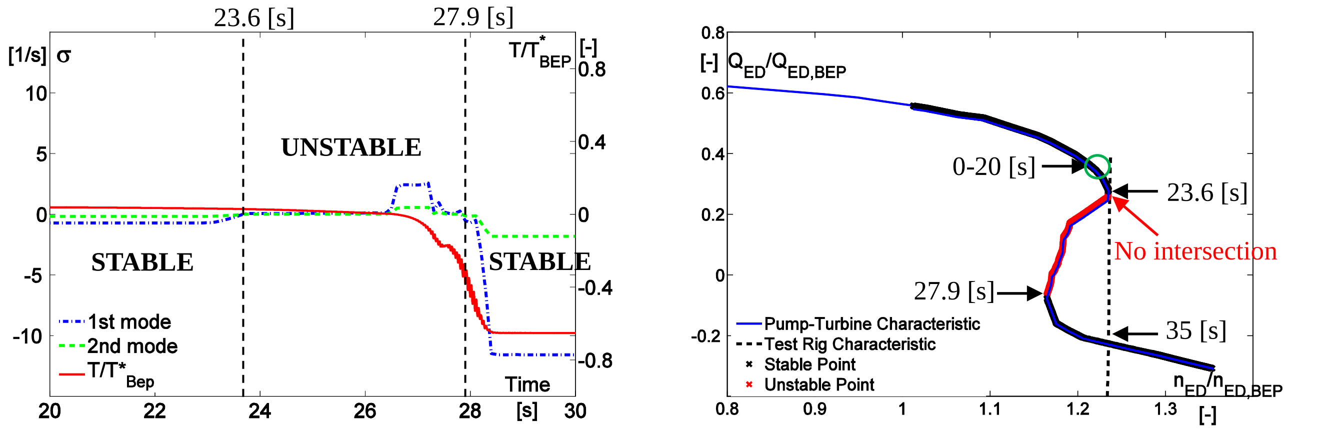

a) Evolution of the real parts for the first two eigenmodes **b)** Stable and unstable zones on the characteristic curve

Fig. 6 Representation of stable operating conditions without the restriction of section

For the case without the restriction of section, the eigenvalue study indicates the presence of unstable operating conditions between 23.6 and 27.9 seconds. This time interval corresponds to the portion of the operating curve where the slope is positive ($dT_{ED}/dn_{ED} > 0$ and $dQ_{ED}/dn_{ED} > 0$) and is highlighted by red symbols in the Fig. 6.b. Moreover, in the present case, the head losses are relatively small compared to the head imposed and therefore test rig characteristic curve is similar to a straight line. Thus, without a restriction of section, the only degree of freedom for the system is the modification of the head H_{pump} created by the pump, imposing a horizontal translation of the test rig characteristic curve (Fig. 7.a). So, by increasing H_{pump}, three new operating points are created. As the change of the head H_{pump} does not influence the definition of stable and unstable operating conditions, it becomes impossible to have a stable operating point in the “S-curve” without a restriction of section. Indeed, among the three operating points, the system will stabilize only at #1 or #2 and never at #3.

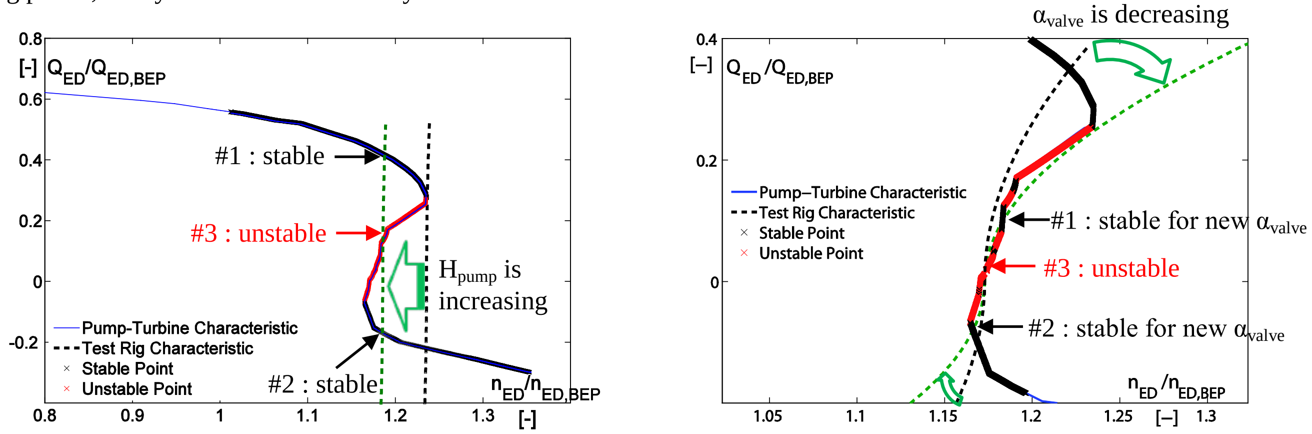

a) If the head H_{pump} imposed by the pump is increased **b)** If the Iris valve opening α_{valve} is decreased

Fig. 7 Evolution of operating points for each of the two degrees of freedom

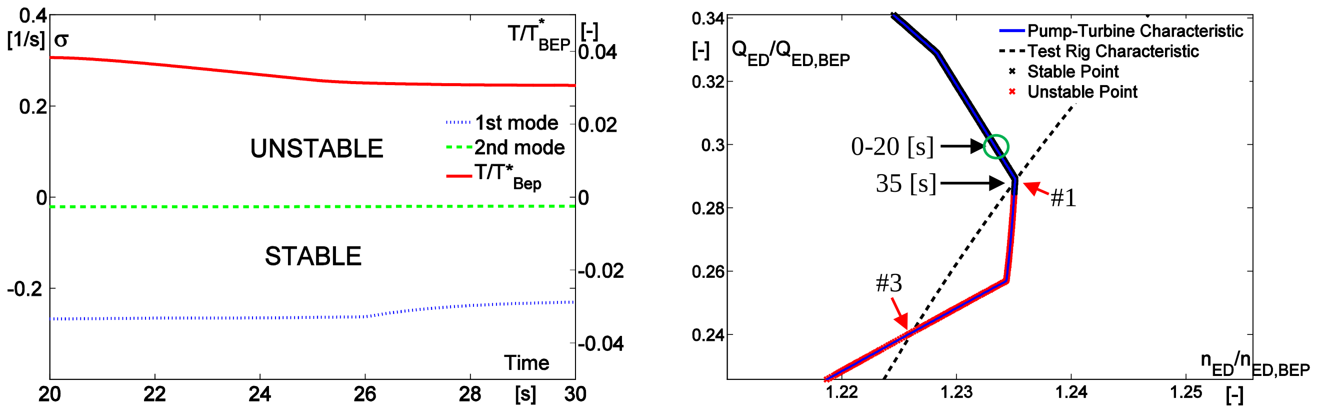

a) Evolution of the real parts for the first two eigenmodes **b)** Stable and unstable zones on the characteristic curve

Fig. 8 Representation of stable operating conditions with the restriction of section

Applying the same analysis to the system with a restriction of section, the real part of the eigenvalues is always negative (Fig. 8.a), confirming the evolution in a stable zone throughout the transitional period. To better visualize the different stable and unstable zones, the Fig. 8.b indicates with black symbols the points where the real part of the eigenvalues is negative. Thus, by increasing the rotational speed, the operating point is shifted from its initial position to the first operating point, remaining in a stable zone. Moreover, the stability analysis confirms the presence of an unstable zone around the point #3 and therefore the inability to stabilize the hydraulic system in this region. Finally, the restriction of section creates a new degree of freedom. Indeed, by changing the Iris valve opening α_{valve}, the stable and unstable zones change and stable operating points can appear in the "S-curve" (Fig. 7.b).

6. Conclusions

The numerical model of the EPFL PF3 test rig simulated with SIMSEN provides extensive information about the dynamic behavior of the pump-turbine. First, the operating points of a pump-turbine system are defined by the solution of the equation relating the test rig characteristic and the energy-discharge characteristic of the hydraulic machine for a given rotational speed and a constant guide vanes opening. Then, an eigenvalue study of the non-linear hydraulic system determines the stability of different points of the operating curve.

Furthermore, without a restriction of section, the system has only one degree of freedom (H_{pump}) and it becomes impossible to have a stable operating point in the "S-curve". However, the addition of a restriction alters the curvature of the test rig characteristic and creates a second degree of freedom (α_{valve}) to achieve stable operating points in the "S-shaped" curve.

Finally, a study of operating points indicates the minimum rotational speed at which the system switches to reverse pumping mode for a given hydraulic configuration. A small loop optimization can determine what would be the minimal restriction of the section to ensure a stable operating point in generating mode.

Acknowledgments

The present investigation was carried out in the frame of HYDRODYNA II project (Eureka N° 4150), in a partnership with ALSTOM Hydro, ANDRITZ Hydro, VOITH Hydro and UPC-CDIF. The authors would like to thank the Swiss Federal Commission for the Technology and Innovation (CTI), Swisselectric Research and the Energy Program of The Ark, the Foundation for Innovation of Valais Canton, for their financial support as well as the HYDRODYNA II partners for their involvement and support.

Nomenclature

A	Cross-section area [m^2]	L	Hydraulic inductance [s^2/m^2]	T_{ED}	IEC torque factor [-]
a	Wave speed [m/s]	n	Rotational speed [rps]	α_O	Guide vanes opening [-]
C	Hydraulic capacitance [m^2]	n_{ED}	IEC speed factor [-]	α_{valve}	Iris valve opening [-]
D	Diameter [m]	Q	Discharge [m^3/s]	λ	Local loss coefficient [-]
E	Specific hydraulic Energy [J/kg]	Q_{ED}	IEC discharge factor [-]	μ_{equ}	Viscoelastic damping [Pa s]
g	Gravity [m/s^2]	R	Hydraulic resistance [s/m^2]	ν	Specific speed [-]
H	Head [m]	R_{ve}	Viscoelastic resistance [s/m^2]	ρ	Density [kg/m^3]
H_{pump}	Head created by the pump [m]	s	Complex eigenvalue [-]	σ_k	Damping [1/s]
K_v	Specific energy loss coefficient [-]	T	Torque [Nm]	ω_k	Oscillation pulsation [rad/s]

References

[1] Warnick, C.C., et al., 1984, "*Hydropower Engineering*", Prentice Hall, pp.44-45.
[2] Martin, C. S., 1986, "*Stability of Pump-Turbines during Transient Operation*", 5th International Conference on Pressure Surges, pp.61-71.
[3] Martin, C. S., 2000, "*Instability of Pump-Turbines with S-shaped Characteristics*", Proceedings of the 20th IAHR symposium on Hydraulic Machinery and Systems.
[4] Dörfler, P.K., Engineer, A.J., Pendse, R.N., Huvet, P. and Brahme, M. V. 1998, "*Stable operation achieved on a single-stage reversible pump-turbine showing instability at no-load*", Proceedings of the 19th IAHR symposium on Hydraulic Machinery and Systems, pp.430-440.
[5] Hasmatuchi, V., Roth, S., Botero, F., Avellan, F. and Farhat, M., 2010, "*High-speed flow visualization in a pump-turbine under off-design operating conditions*", IOP Conf. Series: Earth and Environmental Science 12 (2010) doi:10.1088/1755-1315/12/1/012059.
[6] Wylie, E .B. and Streeter, V.L., 1993, "*Fluid transients in systems*" Prentice Hall, Englewood Cliffs, N.J.
[7] Nicolet, C., Alligné, S., Kawkabani, B., Koutnik, J., Simond, J.J. and Avellan, F., 2009, "*Stability Study of Francis Pump-turbine at Runaway*", 3th IAHR International Meeting of the Workgroup on Cavitation and Dynamic Problems in Hydraulic Machinery and Systems.
[8] Nicolet, C., 2007, "*Hydroacoustic modelling and numerical simulation and unsteady operation of hydroelectric systems*", Thesis EPFL n°3751, Laboratory for Hydraulic Machines, Ecole Polytechnique Fédérale de Lausanne, Switzerland.
[9] Alligné, S., Nicolet, C., Allenbach, P., Kawkabani, B., Simon, J.J., Avellan, F., 2009, "*Influence of the Francis turbine location under vortex rope excitation on the hydraulic system stability*", International Journal of Fluid Machinery and Systems, Vol. 2.